NASA TECHNICAL MEMORANDUM

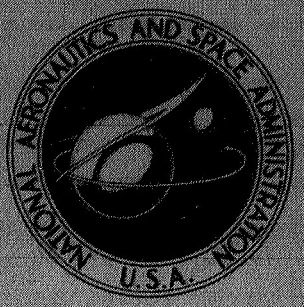

NASA TM X-1756

NASA TM X-1756

EVALUATION OF 7.8-INCH-THROAT-DIAMETER INSERTS AND A UNIQUE COOLING CONCEPT IN A STORABLE-PROPELLANT ROCKET ENGINE

by Jerry M. Winter and Donald A. Peterson

Lewis Research Center

Cleveland, Ohio

NATIONAL AERONAUTICS AND SPACE ADMINISTRATION • WASHINGTON, D. C. • MARCH 1969

NASA TM X-1756

EVALUATION OF 7.8-INCH-THROAT-DIAMETER INSERTS AND A UNIQUE COOLING CONCEPT IN A STORABLE-PROPELLANT ROCKET ENGINE

By Jerry M. Winter and Donald A. Peterson

Lewis Research Center
Cleveland, Ohio

NATIONAL AERONAUTICS AND SPACE ADMINISTRATION

For sale by the Clearinghouse for Federal Scientific and Technical Information
Springfield, Virginia 22151 – CFSTI price $3.00

ABSTRACT

Nominal test conditions were 100 psia (689 kN/m^2) chamber pressure, an oxidant-to-fuel ratio of 2.0, and an initial throat diameter of 7.82 in. (19.8 cm). The propellants were nitrogen tetroxide and a blend of 50 percent hydrazine with 50 percent unsymmetrical dimethyl hydrazine. Magnesium oxide reinforced with metallic honeycomb failed structurally after 60 sec firing duration. A JT0992 (hafnium carbide, silicon carbide, graphite composite) provided nominal erosion protection for 140 sec. A unique active cooling concept was also evaluated. A perforated nozzle wall (liner) was used in conjunction with graphite ribs to conduct heat into an ammonium fluoroborate reservoir surrounding the liner. Three versions of the concept failed either structurally or by excessive throat erosion. These large-size inserts demonstrated less durability than the same materials in a smaller size.

EVALUATION OF 7.8-INCH-THROAT-DIAMETER INSERTS AND A UNIQUE COOLING CONCEPT IN A STORABLE-PROPELLANT ROCKET ENGINE

by Jerry M. Winter and Donald A. Peterson

Lewis Research Center

SUMMARY

Three throat inserts and three versions of a proposed cooling concept were evaluated with a nominal 6700-pound (29 800-N) thrust rocket engine. The throat diameter was 7.82 inches (19.8 cm). Nominal test conditions were 100-psia (689-kN/m^2) chamber pressure and an oxidant-to-fuel ratio of 2.0. The propellants were nitrogen tetroxide and a blend of 50-percent hydrazine with 50-percent unsymmetrical dimethyl hydrazine.

Magnesium oxide reinforced with steel honeycomb and magnesium oxide reinforced with Inconel honeycomb were tested as throat inserts in an ablative thrust chamber. In both cases, structural failure led to erosion after 60 seconds firing duration.

A JT0992 (hafnium carbide, silicon carbide, graphite composite) throat insert provided nominal erosion protection for 140 seconds. Erosion due to oxidation increased rapidly after this time. Structural failure also occurred during the test but did not significantly affect the erosion results.

A unique active cooling concept was also evaluated. A perforated nozzle wall (liner) was used in conjunction with graphite ribs to conduct heat into an ammonium fluoroborate reservoir surrounding the liner. Ammonium fluoroborate coolant gases generated by heat conduction were to pass through the perforated liner into the combustion stream to keep the liner material below its oxidation temperature, thus preventing throat erosion. Three versions of the concept failed either structurally or by excessive throat erosion. It appeared that the cooling affect was inadequate to protect the nozzle liner from the high-velocity corrosive combustion environment.

INTRODUCTION

Reinforced ablative plastics have been used effectively in both liquid- and solid-propellant rocket-engine thrust chambers at all thrust levels. Simplicity, reliability,

and tolerance to deep throttling are factors that make ablative thrust chambers attractive to design engineers. Because throat erosion can cause a performance decrease or alter the thrust vector, it is desirable to maintain a constant throat area during the firing. Performance degradation, resulting from a large percent increase in the throat area, is most severe for small reaction control engines and may be significant for larger engines where maximum efficiency and long duration firings are required. Improvement of the erosion resistance of reinforced plastic ablative materials is under investigation by several organizations (refs. 1 to 4).

Although adequate throat life may eventually be attained with intensive work on improved ablatives, the necessary low erosion rate may also be possible by the use of hard throat inserts. A satisfactory throat insert would provide erosion resistance and maintain structural integrity over an extended and varied duty cycle. An experimental investigation to develop and evaluate throat inserts for small-scale engines (1.2-in. or 3.05-cm throat diam) was reported in references 5 and 6. Large-scale (7.8-in. or 19.8-cm throat diam) insert development and evaluation was reported in reference 7. The results of references 6 and 7 indicated that the use of composite structures would best combine erosion resistance with structural integrity for throat inserts.

Based on these results, three passive composite material combinations were selected for evaluation as throat inserts in large-scale engines. An active cooling concept was also selected for evaluation as another method for eliminating nozzle throat erosion because experience (ref. 7) indicated the difficulty of scaling passive throat insert-material design combinations from 1.2-inch (3.05-cm) diameter to 7.82-inch (19.8-cm) diameter.

The objectives were to eliminate throat erosion and to provide structural integrity over a 700-second duty cycle including multiple restarts. A secondary objective was to obtain scaling information relating behavior of large-scale composite-material inserts to that of small-scale inserts of the same material. The passive throat inserts were composed of various materials for which the physical properties of the composite were not completely known. Therefore, these designs were necessarily based more on previous results and experience in both engine sizes (1.2- and 7.8-in. or 3.05- and 19.8-cm throat diam) than on precise theoretical analyses. For the actively cooled nozzle design, a complete thermal and stress analysis was performed by the manufacturer using the best available material properties to aid in the design and to correlate with experimental results so that modifications could be based on both theory and experiment.

Three throat-insert designs were tested. These were (1) magnesium oxide reinforced with 1010 steel honeycomb, (2) magnesium oxide reinforced with Inconel honeycomb, and (3) JT0992, a composite of hafnium carbide, silicon carbide, and graphite (HfC, SiC, and C). The active cooling concept included (1) use of ammonium fluoroborate, in a reservoir surrounding the nozzle, as a source of coolant gases, (2) perforated nozzle

walls (liners) to provide a path for the coolant gases from the reservoir through the perforations into the nozzle boundary layer, and (3) heat paths (e.g., graphite ribs) to conduct heat from the nozzle liner into the coolant reservoir in order to generate coolant gases. Three versions of the active cooling concept were tested, each modification being based on test results of the pervious design. Two of the versions used a perforated graphite liner with a tantalum carbide (TaC) coating on the combustion gas side. The third version used a tungsten-silver perforated liner with copper foam as the coolant.

The propellants used for the test series were nitrogen tetroxide and a blend of 50-percent hydrazine with 50-percent unsymmetrical dimethyl hydrazine. Nominal test conditions included a chamber pressure of 100 psia (689 kN/m^2) and an oxidant-to-fuel ratio of 2.0. The characteristic velocity efficiency was 97 percent of theoretical equilibrium or above, so that results would be meaningful for a high-performance system. The duty cycle goal was 700 seconds total including two 300-second continuous firings with multiple restart capability. A nozzle expansion area ratio of 1.4 used with a 7.82-inch (19.8-cm) throat diameter provided a nominal vacuum thrust level of 6700 pounds force (29 800 N). A low expansion area nozzle was used to expedite fabrication and evaluation of throat materials.

Each configuration is discussed in detail. Comparisons among tested materials and with previous work are made. Failure mechanisms are discussed and recommendations for improvements are included.

APPARATUS

FACILITY

The investigation was conducted in an altitude chamber of the Propulsion Systems Laboratory. The overall arrangement of the facility is shown in figure 1. Figure 2 illustrates the mounting of a thrust chamber in the test stand. The weight of the chamber was supported by flexure plates that allowed axial freedom of motion for thrust measurement. Engine exhaust products were passed through a water-cooled collector and cooled by heat exchangers before being exhausted through rotating machinery to the atmosphere.

Figure 3 is a flow system diagram and shows measured variables. Two flowmeters in series were used in each propellant line. The propellant tanks were located external to the test cell in a controlled temperature environment (fig. 1). Propellant capacity was sufficient to provide 300 seconds of continuous firing.

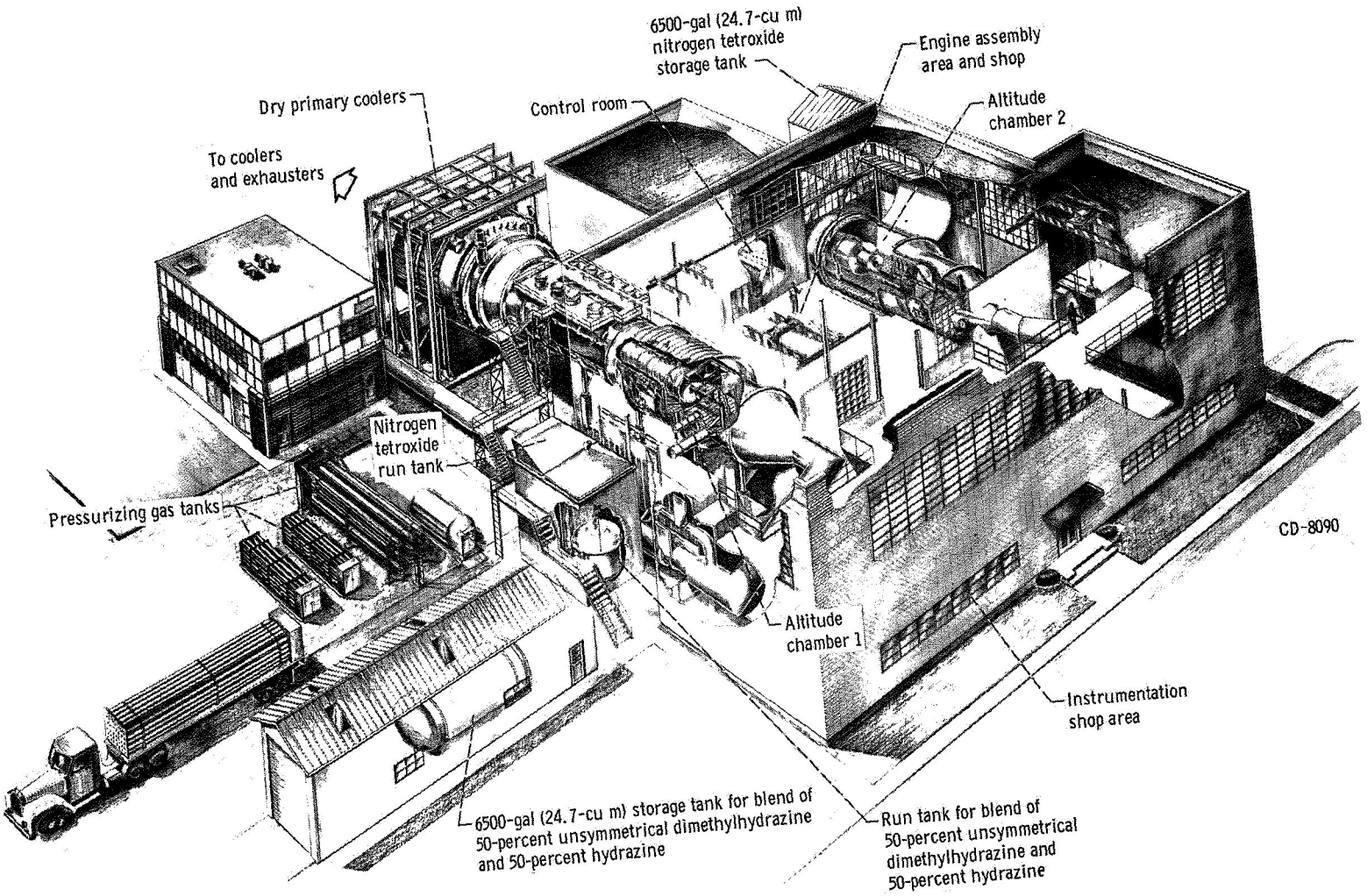

Figure 1. - Altitude facility.

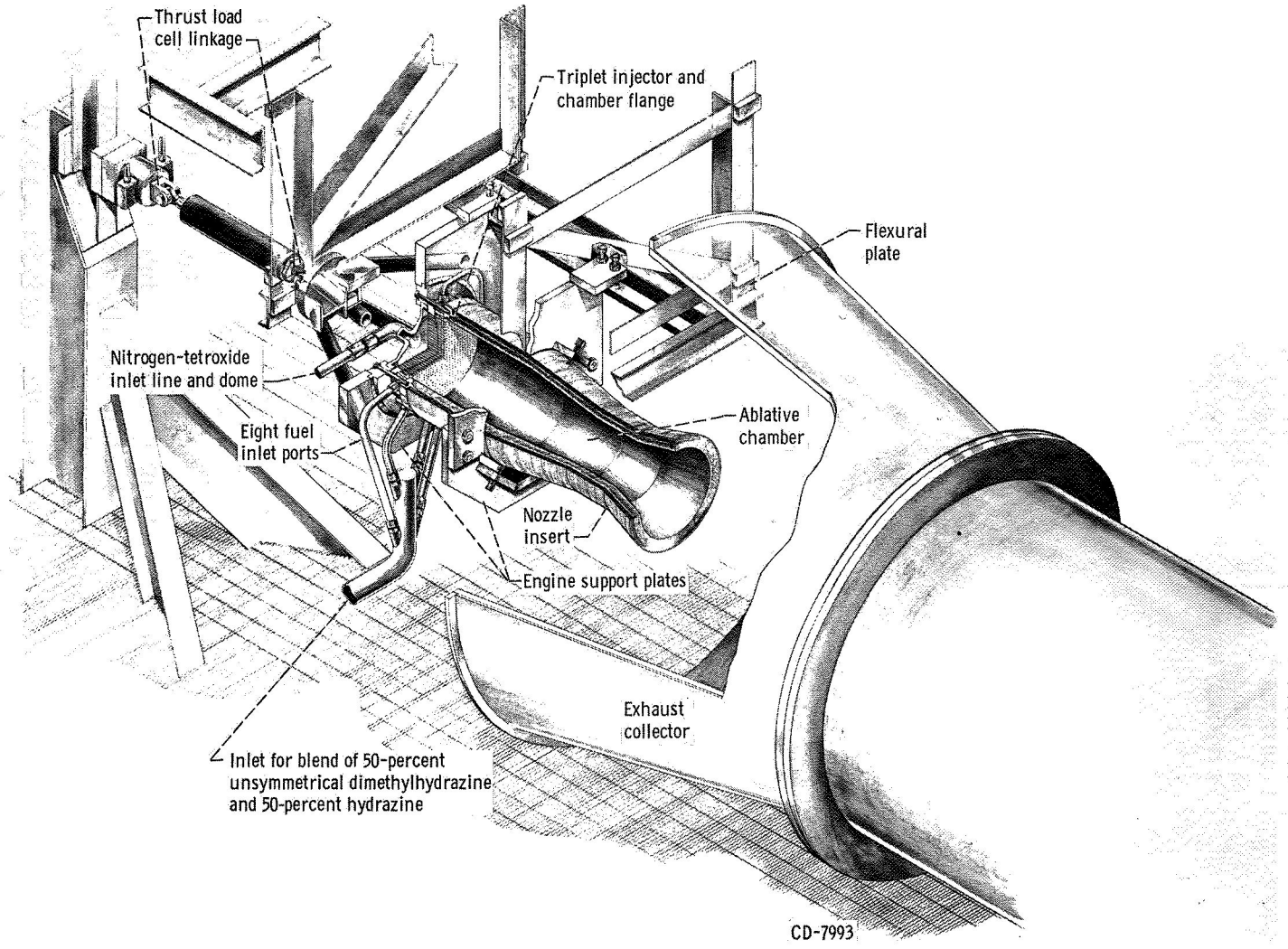

Figure 2. - Ablative chamber and injector; general engine test arrangement.

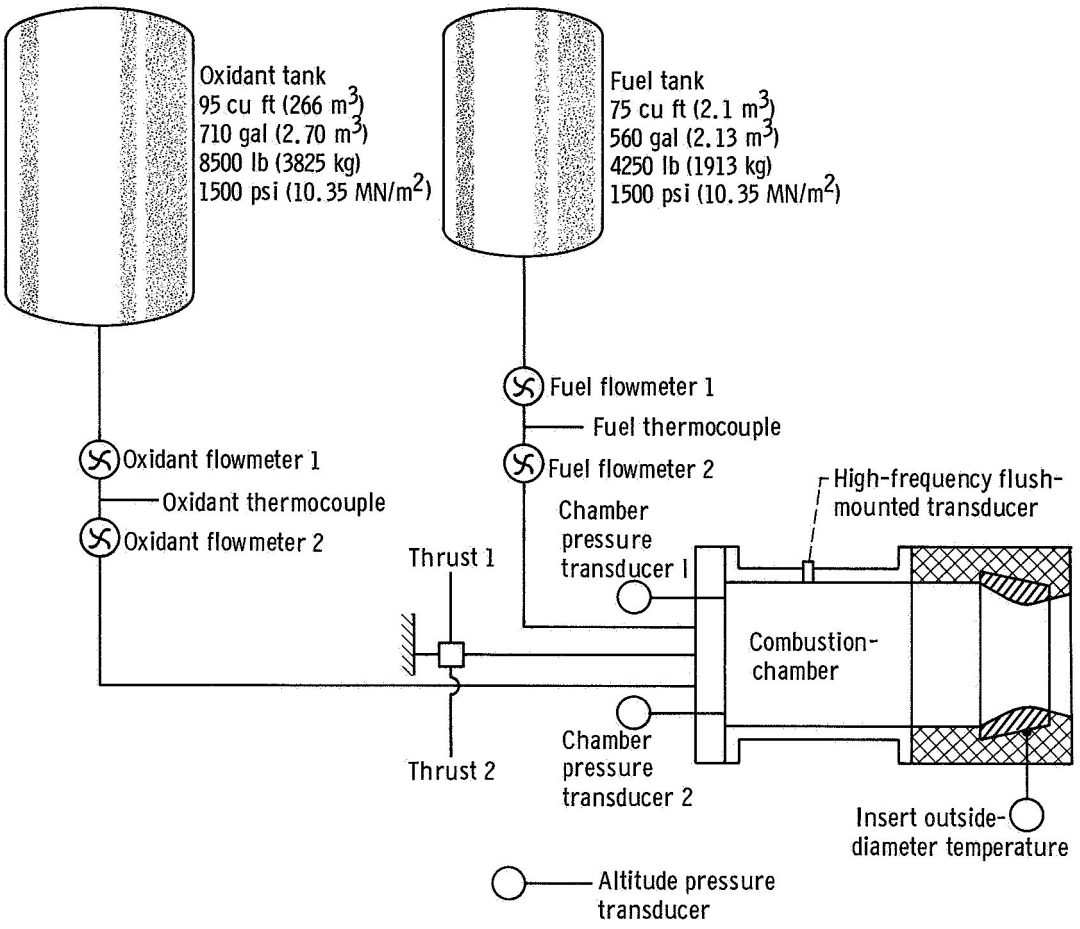

Figure 3. - Flow diagram and instrumentation.

ROCKET-ENGINE ASSEMBLY

Use of a single injector was desired but injector lifetime was limited and required the use of four injectors for the test program. A description of each injector is given in table I. All four injectors were circular pattern fuel-on-oxidant triplet designs. Injector 1 (fig. 4) had all the triplet elements oriented radially. Injector 2 (fig. 5) had the elements in the inner four rows oriented alternately radially and tangentially. The elements in the outer three rows were all radial. Injectors 3 and 4 (fig. 6) had 24 triplets arranged at a 40^{o} angle to the chamber radius with the remainder arranged radially.

A sketch of the rocket-engine assembly, together with the specific dimension for each thrust chamber assembly tested, is given in table II. Detailed sketches and dimensions for each throat insert and cooling concept are given in the Results and Discussion

TABLE I. - INJECTOR DESCRIPTION

[Pattern, circular; design, fuel-on-oxidant triplets; face material, aluminum, impingement distance, 0.56 in. (1.42 cm); impingement included angle, 40°.]

Injector	Oxidant holes			Fuel holes			Triplet orientation
	Number	Size		Number	Size		
		in.	cm		in.	cm	
1	127	0.07850	0.199	254	0.043	0.109	Radial
2	31	0.0595	0.151	62	0.038	0.097	Radial
	60	.0595	.151	120	.038	.097	Tangential
	144	.025	.064	288	.016	.041	Radial
3 and 4	103	0.0785	0.199	206	0.043	0.109	Radial
	24	.0785	.199	48	.043	.109	40° to Radius

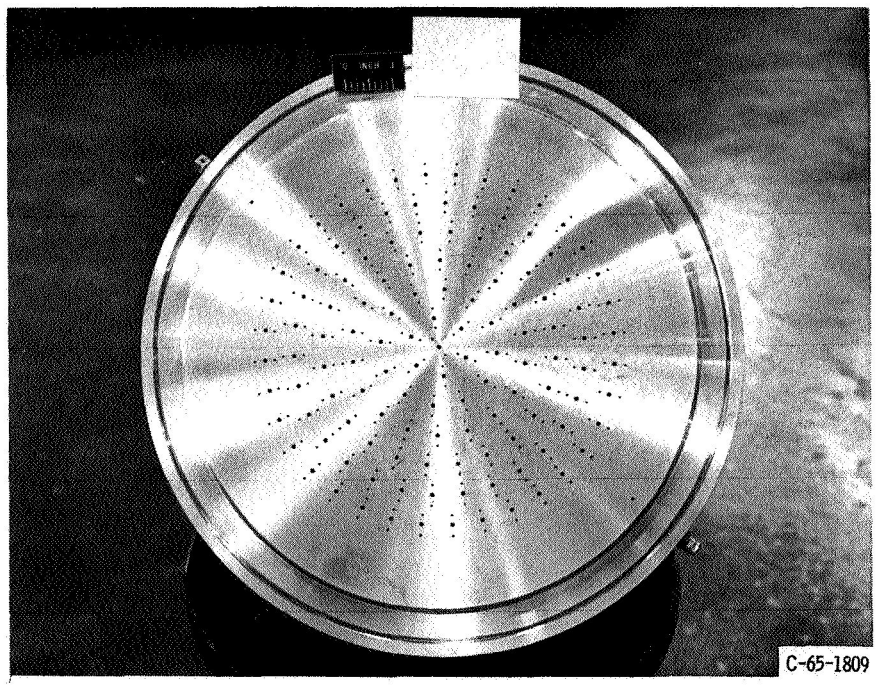

Figure 4. - Injector 1.

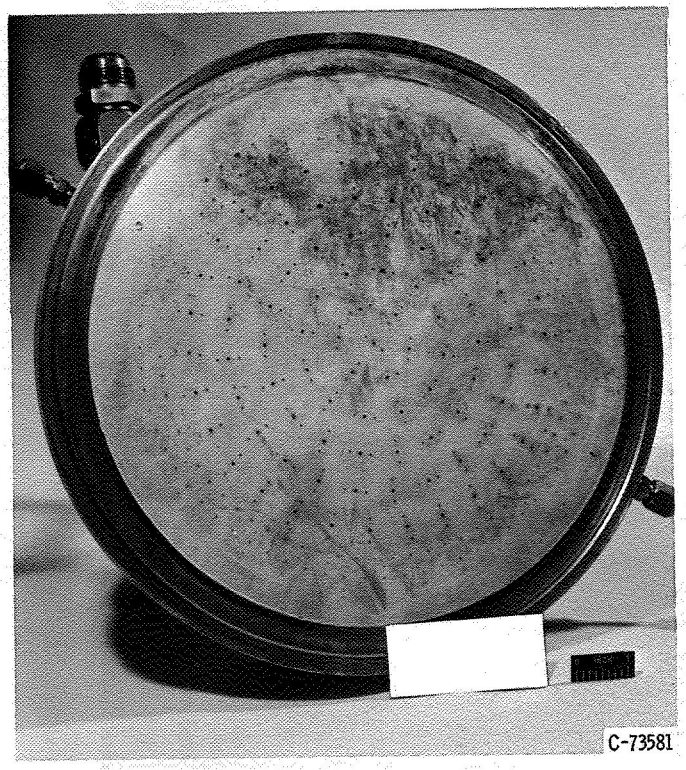

Figure 5. - Injector 2.

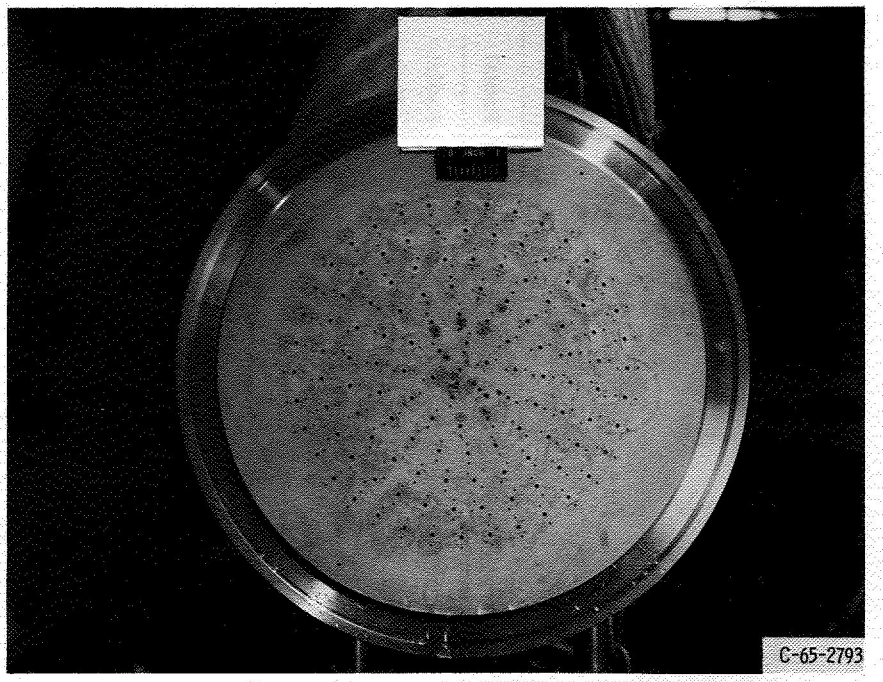

Figure 6. - Injectors 3 and 4.

TABLE II. - ROCKET-ENGINE DIMENSIONS

[Water-cooled chamber diameter, D_{wc}, 10.78 inches (27.35 cm).]

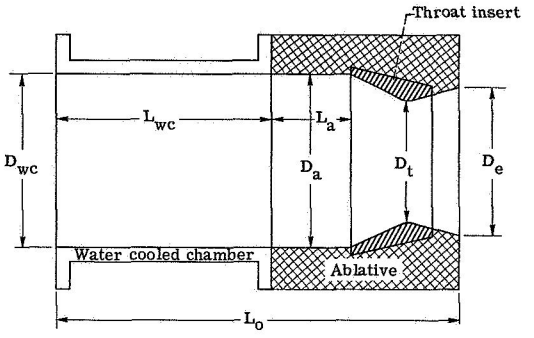

Nozzle	Type	Water-cooled chamber length, L_{wc}		Ablative diameter, D_a		Length, L_a		Throat insert diameter, D_t		Nozzle exit diameter, D_e		Total physical length, L_o		Nozzle expansion area ratio, ϵ	Characteristic chamber length, L*	
		in.	cm	in.	cm	in.	cm	in.	cm	in.	cm	in.	cm		in.	cm
1	Insert 1	12.0	30.45	10.86	27.60	6.28	15.95	7.84	19.90	9.35	23.7	25.7	65.3	1.42	40.33	102.5
2	Insert 2	12.0	30.45	10.86	27.60	6.28	15.95	7.82	19.84	9.36	23.75	25.7	65.3	1.43	40.55	103.0
3	Insert 3	12.9	32.75	10.78	27.35	6.52	16.52	7.83	19.87	9.28	23.35	25.7	65.3	1.40	42.36	107.5
4A	Cooling concept A	20.0	50.75	None	None	None	None	7.82	19.84	9.40	23.85	25.5	64.75	1.48	43.24	110.0
4B	Cooling concept B	20.9	53.10	None	None	None	None	7.82	19.84	9.40	23.85	26.4	67.0	1.48	44.95	114.0
4C	Cooling concept C	20.9	53.10	None	None	None	None	7.82	19.84	9.40	23.85	26.4	67.0	1.48	44.95	114.0

section. Performance was evaluated using both zirconium oxide coated steel thrust chambers and water-cooled thrust chambers.

INSTRUMENTATION

The location of all measured variables is shown in figure 3. Pressure measurements were made with strain-gage element transducers. A high-frequency flush-mounted crystal transducer was used to monitor for combustion instability. Electrical calibrations were made before and after each test with the use of calibration information from laboratory standard tests. Thrust measurements were made with a double-bridge strain-gage load cell in compression. Calibration was accomplished by loading the thrust cell hydraulically with the engine in place and measuring the true load with a proving ring calibrated by the National Bureau of Standards. Propellant flows were measured with turbine flowmeters. Calibrations from water-flow measurements were used for the fuel meters, and calibrations obtained with nitrogen tetroxide flow were used for the oxidant meters. Propellant-flow temperatures were measured with iron-constantan thermo-

couples referenced to a 150° F (340 K) oven. Insert wall temperatures were measured with tungsten - tungsten-rhenium thermocouples referenced to ambient temperature.

PROCEDURE

ENGINE OPERATION AND CONTROL

The altitude chamber pressure was set at 1.74 psia (12.0 kN/m^2) prior to each firing. This level was selected to match the facility altitude capability to the engine flow rate so that no significant altitude change occurred during the test firing. The propellant tanks were pressurized with nitrogen gas. An automatic closed-loop controller was set to provide a constant chamber pressure of 100 psia (689 kN/m^2). A second closed-loop controller was set to provide a constant oxidant-to-fuel ratio of 2.0 for the duration of each firing. Thus, if throat erosion occurred, the propellant flow rate was increased to maintain constant chamber pressure. The firing time was determined by throat erosion or by an arbitrarily selected time. A high-frequency flush-mounted pressure transducer located on the chamber was monitored with an oscilloscope. Firing was terminated immediately if high-frequency combustion oscillations were observed.

At regular intervals through the program, test firings were made to calibrate injector performance. For these calibration tests, run durations were 6 seconds. Zirconium oxide coated heat-sink engines and water-cooled engines were both used for performance calibrations.

DATA RECORDING AND PROCESSING

The electrical transducer outputs were sampled at the rate of 4000 samples per second. The outputs were digitized and recorded on magnetic tape by a central data-recording system. Selected transducer outputs were also recorded in analog form by multichannel oscillograph and strip-chart recording instruments for use in monitoring system operation. The primary digital data were converted into calculated values by use of a digital computer.

The symbols and calculations used are listed in the appendix. The primary method for calculating the effective throat radius change ΔR_e was as follows:

$$\Delta R_e = R_t - R_i$$

where the initial radius R_i is that determined by micrometer measurement of the throat

insert before any testing. The throat radius R_t was calculated during each firing using the following equation and assuming constant ηC^* as determined from calibration firings:

$$R_t = \sqrt{\frac{(\eta C^*)(C^*_{theo})(W_p)}{\pi(g)(P_{c,corr})(C_d)}}$$

To check the calculation, the throat diameter was measured at 45^o intervals with a micrometer following testing. The values were converted to effective throat radius change by subtracting the initial throat radius.

RESULTS AND DISCUSSION

COMBUSTION ENVIRONMENT

The characteristic velocity efficiency C^* of each injector is listed in table III. The values were obtained from thrust measurements by the calculation methods given in the appendix. The precision of the C^* values is also listed in table III in terms of the 3σ variation. The number of calibration firings and nozzle test firings is also listed in table III. All the passive throat inserts were tested with injector 1 and were subjected to the same combustion environment. Injectors 2, 3, and 4 were used in tests of the three actively cooled nozzles. Three different injectors were required because their use on other test programs caused failure which prevented use of a single injector. Unpublished heat-transfer measurements indicate that the three injectors used were similar, so that

TABLE III. - INJECTOR PERFORMANCE

Injector	Number of calibration firings	Characteristic exhaust velocity efficiency, ηC^* percent	ηC^* Precision[a], percent	Nozzle test firings		
				Nozzle	Number of firings	Total time, sec
1	18	97.2	±0.5	1, 2, and 3	6	546
2	7	98.2	±1.9	4A	1	30
3	17	97.0	±1.2	4B	1	98
4	8	97.0	±.8	4C	1	166

[a] 3σ for 99 percent of data.

the results of the nozzle evaluations were not affected by the use of different injectors.

Injectors were evaluated using both zirconium oxide coated steel thrust chambers and complete water-cooled thrust chambers. No significant difference in performance was measured between these two cases.

THROAT INSERT RESULTS

A complete profile of each insert is given including design, throat erosion, and a post-test photograph. Each insert is discussed in terms of design, firing results, post-test analysis, comparison with small-scale testing, and correlation with theoretical calculations.

Honeycomb Reinforced Magnesium Oxide

In general, oxides provide the required oxidation resistance in the storable-propellant combustion environment. Oxides that do not melt in the combustion environment generally fail structurally, however. Various methods that are useful in preventing structural failure are available and one (honeycomb reinforcement) has been used successfully in nose-cone applications. Magnesium oxide (MgO) with mild steel honeycomb and with Inconel honeycomb was selected to evaluate the performance of these composites in large-scale throat inserts. Previous experience with small-scale insert testing (ref. 6) had indicated thermal stress failure but no throat erosion over a 200- to 300-second firing. It was recognized that the mild steel and Inconel might melt on the inside surface of the insert, but it was hoped that enough of the honeycomb structure would remain to prevent loss of the magnesium oxide if cracking occurred. Experience with nose-cone fabrication indicated that structures using these particular materials could be fabricated efficiently and economically.

Magnesium oxide reinforced with mild steel honeycomb; insert 1. - Figure 7 shows the throat insert prior to installation and test. X-ray examination determined that the structure was sound and free of voids. However, the honeycomb structure was distorted by the sintering and pressing operation required to make a high-density structure.

The nozzle design is shown in figure 8(a). Magnesium hydroxide-phenolic was selected as the ablative chamber material to eliminate the possibility of a reaction between the MgO and molten silica from silica-phenolics normally used. The nozzle with the throat insert was tested downstream of a water-cooled chamber section.

The test firing results in terms of throat erosion are given in figure 8(b). The test was ended after 83 seconds because of a gas leak in the chamber section. The ablative

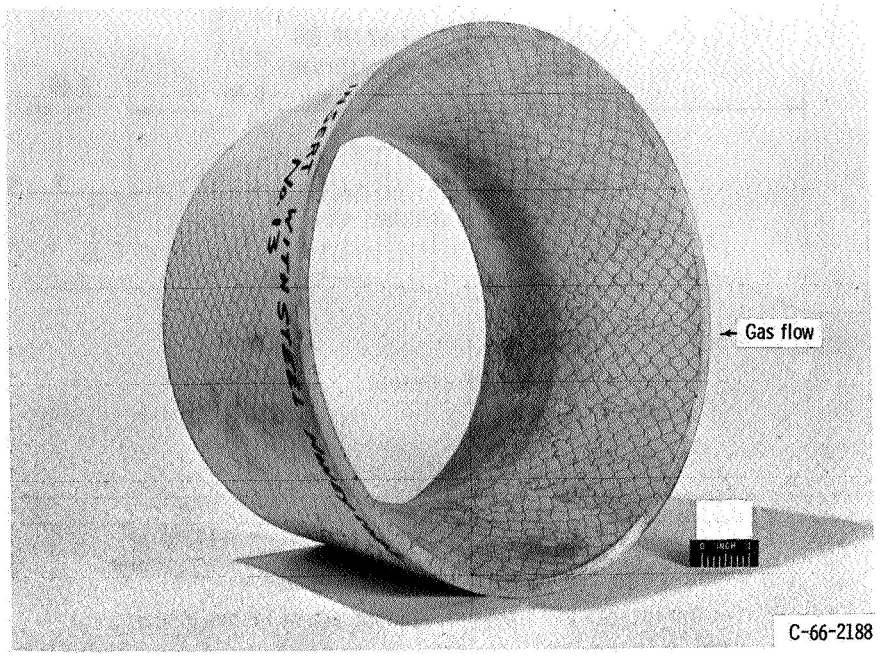

Figure 7. - Insert 1; magnesium oxide with mild steel.

material cracked, allowing combustion gases to escape (see upper left of fig. 8(c)). Figure 8(c) also shows the radial layered structure of the insert following testing. One layer had been partially removed because of cracking, which caused the rapid increase in erosion after 60 seconds of firing time. As expected, there was no chemical reaction observed between the magnesium hydroxide-phenolic and the throat insert; however, cracking of the ablative material allowed hot-gas leakage. The test was terminated when gas leakage was detected.

Comparison with the test results of small-scale inserts using the same materials can be made with the results reported in reference 6. A similar layered structure was observed after testing but the layer was not removed from the surface in the small-scale tests. Loss of the cracked layer in the large-scale insert illustrates the difficulty of scaling complex materials. The honeycomb reinforcement was adequate in preventing material loss in the small-scale but was not adequate at the larger scale. No theoretical stress calculations were made because the material properties of the composite insert were unknown.

Magnesium oxide reinforced with inconel honeycomb; insert 2. - Insert 2 was similar in appearance to insert 1 (fig. 7) prior to test. The nozzle design shown in figure 9(a) was also similar. A silica-phenolic ablative material was used with insert 2 to prevent the ablative material structural failure experienced with magnesium-hydroxide phenolic used with insert 1 (thought to be a greater problem than $MgO\text{-}SiO_2$ reaction).

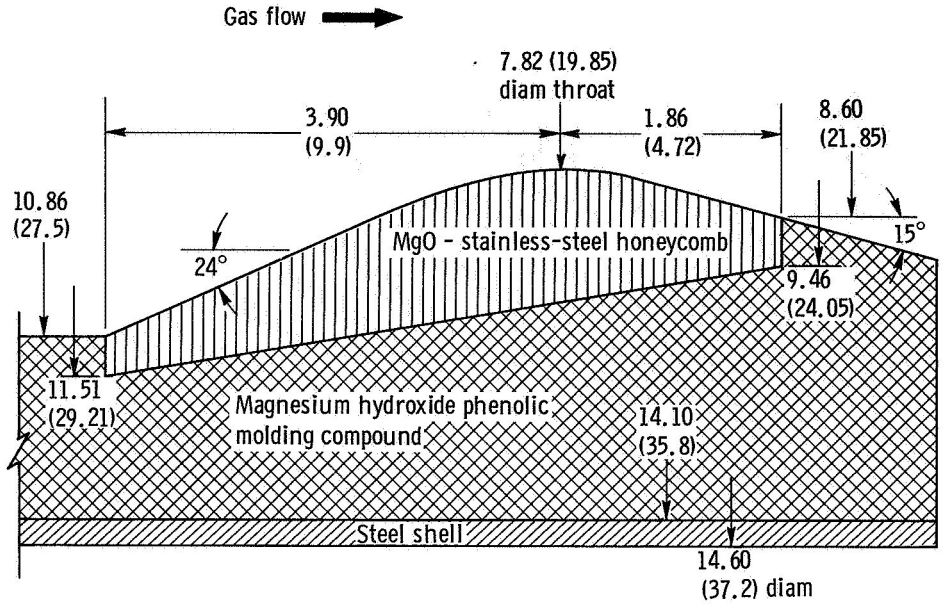

(a) Insert. (All linear dimensions are in inches (cm).)

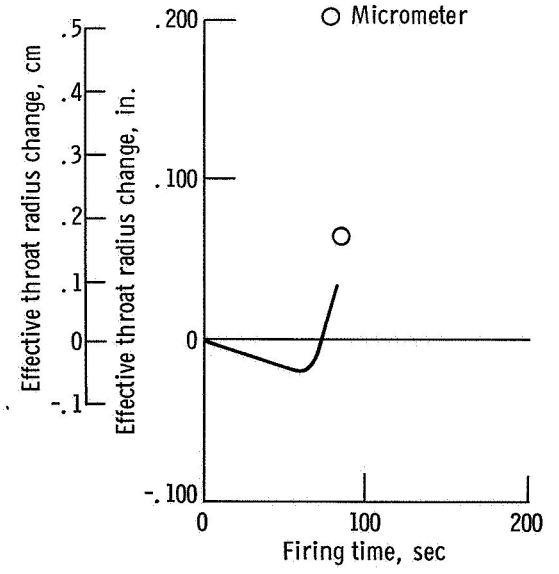

(b) Throat erosion.

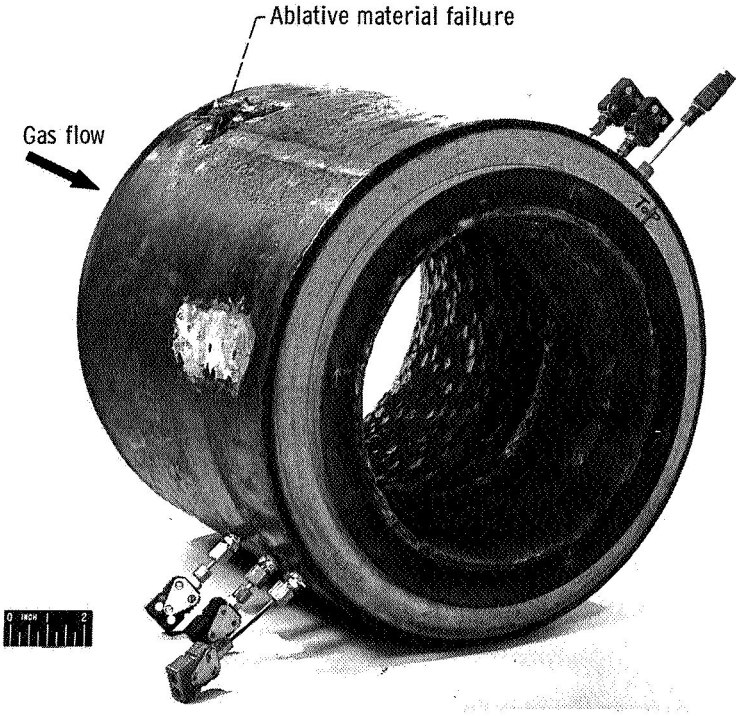

C-66-2641

(c) Post-test photograph.

Figure 8. - Profile of insert 1.

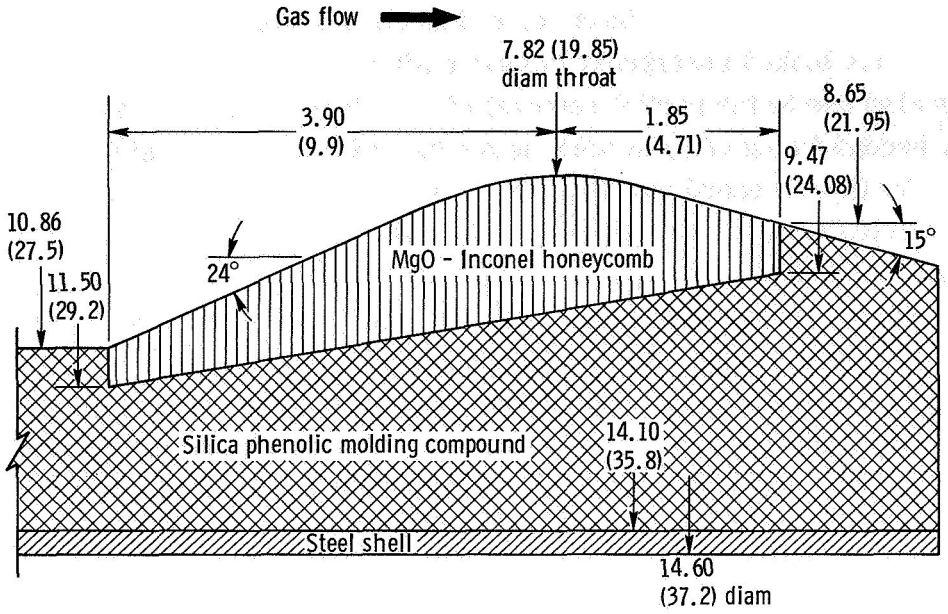

(a) Insert. (All linear dimensions are in inches (cm).)

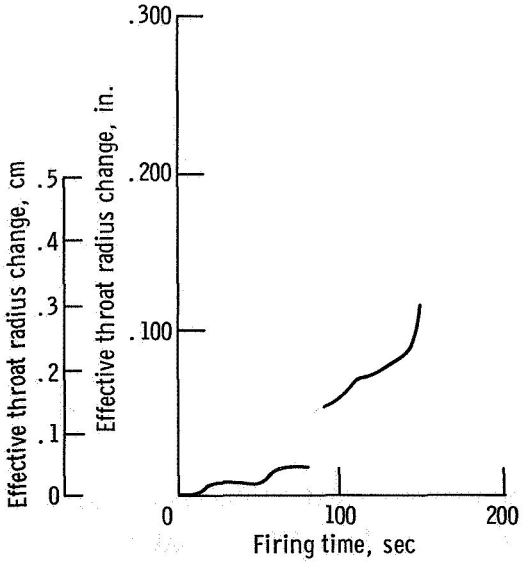

(b) Throat erosion.

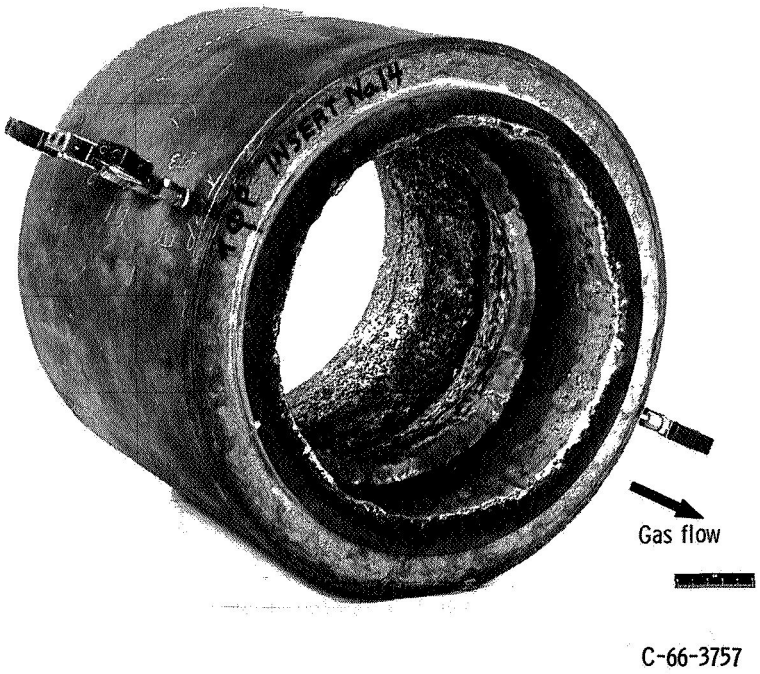

(c) Post-test photograph.

Figure 9. - Profile of insert 2.

The test firing results are given in figure 9(b). The first firing was ended after 80 seconds in order to compare the behavior of inserts 1 and 2 after the same firing duration. Both inserts looked essentially the same after the first firing, and the erosion of insert 2 was also due to the partial removal of a surface layer as was the case with insert 1. A second firing of 78 seconds was ended when throat erosion, due to structural failure of the MgO, increased rapidly. Once the final failure mode and its rate of progression was established, the test was terminated to preserve enough of the insert to perform a post-test examination.

The post-firing photograph of figure 9(c) shows extensive loss of material from the downstream end of the insert. All the insert material is missing from the throat plane to the exit end, probably due to circumferential cracks. Reaction with the silicon dioxide at the insert leading edge was not severe although several pieces were missing from the leading edge because of structural cracking. The final failure mode after removal of the initial layer was caused by radial cracks extending completely through the ceramic and its reinforcement. The composite was not strong enough to withstand the applied thermal stress.

Loss of the insert trailing edge had also been experienced in the small-scale testing. The extent of the failure and its progression were less severe in the small-scale insert (see ref. 6). No theoretical stress calculations were made for insert 2 also because of a lack of adequate material property data.

Summary of reinforced magnesium oxide inserts. - Throat erosion due to structural failure was not eliminated by reinforcing MgO with mild steel or Inconel honeycomb. Although identical modes of thermal stress failure were present in both large- and small-scale inserts, loss of material began sooner and was more severe in the large-scale inserts. Recently completed work on the small-scale inserts indicates better materials are available (ref. 6). Better refractory-metal - oxide matrix combinations should be selected from the later small-scale development testing. Variables that could be controlled to provide better performance in large-scale honeycomb reinforced inserts could include insert wall thickness, honeycomb cell size, and metal thickness. For a limited test effort, emphasis should be placed on methods for dispersing the reinforcement more uniformly throughout the oxide by use of smaller cells and thinner metal.

JT0922 Carbide-Graphite Composite; Insert 3

Carbides, in general, oxidize in the storable-propellant combustion environment, and also may fail structurally because of thermal stress (ref. 6). The JT0992 material is a composite of hafnium carbide - silicon carbide (HfC - SiC) and graphite. The graphite was added primarily to reduce possibility of thermal-stress failure. It was hoped that the

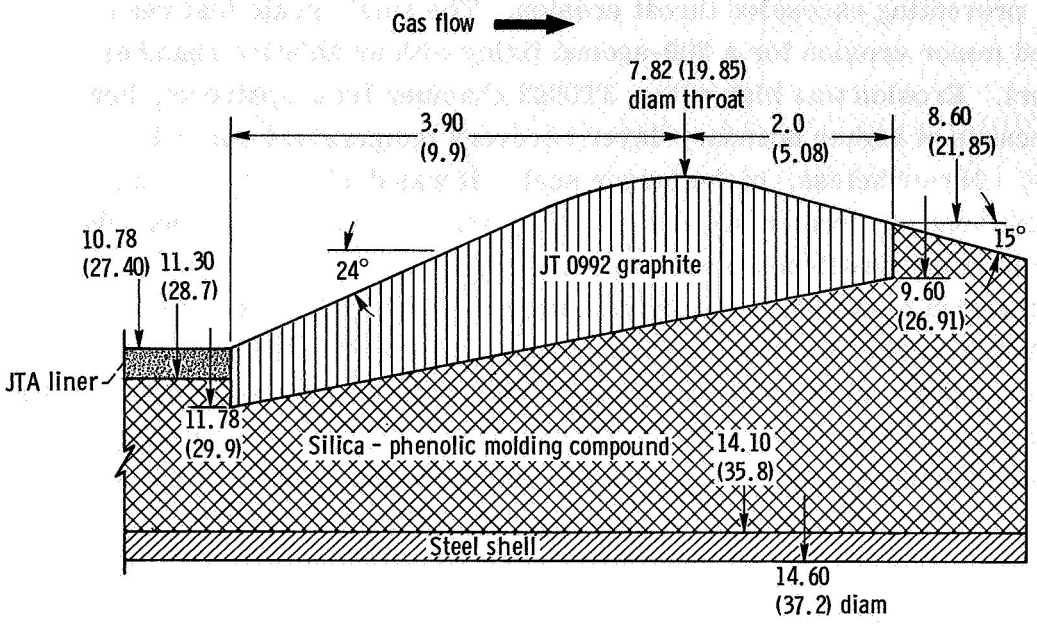

(a) Insert. (All linear dimensions are in inches (cm).)

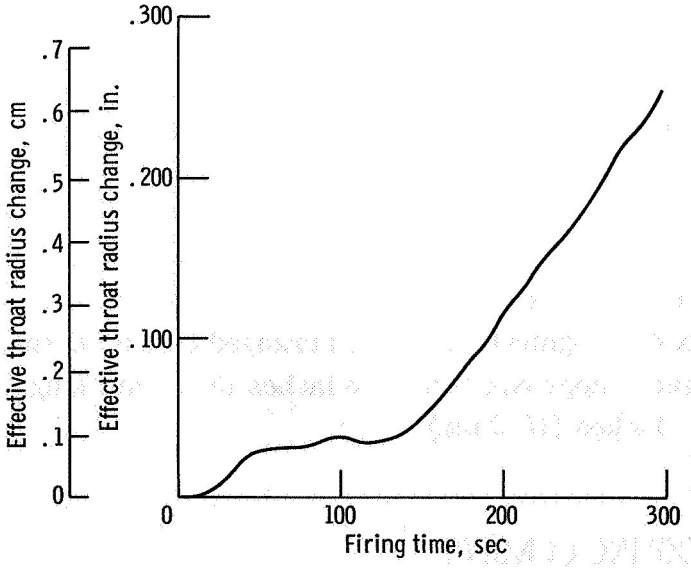

(b) Throat erosion.

C-67-3019

(c) Post-test photograph.

Figure 10. - Profile of insert 3.

oxidation products (HfO_2 and SiO_2) would form a protective coating on the insert surface thereby preventing excessive throat erosion. The small-scale test results in reference 6 indicated minor erosion for a 300-second firing with an ablative chamber upstream of the insert. Erosion was high with a JT0992 chamber liner upstream, however (apparently because of higher boundary-layer recovery temperature without the upstream ablative). Nevertheless, in the larger scale, it was decided to use a JTA chamber liner to prevent ablative erosion at the chamber-insert interface as had been done successfully with many of the small-scale nozzles of reference 6.

The design of the nozzle is shown on figure 10(a). The upstream liner of JTA was made as thin as possible to minimize thermal stress. The firing results in terms of throat erosion are given in figure 10(b). The magnitude of erosion after approximately 140 seconds indicates that the oxidation products formed on the surface did not have sufficient adhesion and were removed as rapidly as they formed. Post-test inspection revealed that the JTA liner had been completely removed. Inspection of the oscillograph data revealed an excursion in chamber pressure after 5 seconds of firing. This pressure excursion could have been caused by pieces of the JTA liner passing through the nozzle throat following structural failure. The post-test photograph of figure 10(c) illustrates the severity of cracking of the insert as well as the patches of nonadherent oxide formed during firing.

The structural failure of both the JTA liner and the JT0992 insert was unexpected in light of experience with these materials in the small-scale program of reference 6. The difference could be due to weaker physical properties formed during the manufacture of large components or higher stresses in the larger size. The throat erosion rate (1.0 mil/sec (0.0025 cm/sec)) was similar to the erosion rate in the small-scale program with the JT0992 insert tested using a JT0992 chamber liner upstream. The lack of adherence of the protective oxide could have been influenced by many factors including the applied shear stress, the constituents formed during oxidation, and the exact temperature of the combustion products.

The number and location of the cracks which were noted after the firing may be instructive for future design. A review of figure 10(c) would indicate that for this size insert, a segmented concept might be successful in eliminating cracking due to thermal stress. Based on the test experience, six 60° segments could be arranged circumferentially. Four axial rows of six segments each, approximately 1.5 inches (3.81 cm) long, would be required for an insert length of 6 inches (15.2 cm).

UNIQUE COOLING CONCEPT

To provide an alternate approach to elimination of throat erosion over an extended

duty cycle of 700 seconds firing, an active cooling concept was considered. The concept included the use of a perforated liner as the basic throat structure. Around the liner, graphite ribs were used to conduct heat radially and help support the liner. A gas-generating solid, ammonium fluoroborate (NH_4BF_4), was contained within the cavities or bays formed by the ribs (see fig. 10). The concept depended on the heat input from combustion to cause the solid to sublime. The design intent was that the gases derived would then be forced through the perforated liner into the combustion gas stream in sufficient quantity to keep the temperature of the liner below the oxidation threshold temperature for the particular liner material selected. The originator of the concept and supplier of the nozzle (Emerson Electric Co.) made a detailed thermal and structural analysis to aid in the nozzle design. Unpublished data from the supplier included the methods of computation, and the theoretical results for each of three different nozzle designs. The three nozzles tested were run in an interrupted series so that the experience gained during testing could be used to design the succeeding nozzles.

Tantalum Carbide Coated Perforated Graphite Liner; Nozzle 4A

The design of nozzle 4A is illustrated in figure 11. The holes in the liner were arranged over the cavities where the coolant material was placed. The design porosity was 10 to 11 percent of the total liner surface area. A 0.004-inch (0.0102-cm) thick TaC coating was used on the graphite (ATJ grade) liner to assist in oxidation protection. A photograph of the liner before assembly is given in figure 11(b). The temperature and stress analyses indicated the design should perform satisfactorily over a 700-second firing duration. The difficulty of making these predictions realistically can be appreciated when the complexity of the design is seen.

The test firing of nozzle 4A was programmed for 30 seconds to evaluate the structural integrity of the design as well as the short-term thermal performance. The 30-second firing produced no appreciable throat erosion. Post-test inspection revealed one circumferential crack in the liner between the 11th and 12th row of holes (counting from the upstream end toward the throat) directly over coolant bay 6. There were also three axial cracks in the upstream portion of the liner. See figure 11(c) for a post-test photograph of the cracked liner. Figure 11(c) also shows the amount of coolant depleted from bay 6 after the firing.

In figure 11(d), the manufacturer's predicted sublimate recession is compared with that measured in bay 6 after the 30-second firing. Bay 6 showed the maximum recession possibly because the circumferential crack in the liner was also in bay 6. The temperatures measured on the outside of the liner (fig. 11(d)) were 2200° F (1200° C) lower than the predicted values. Based on the measurements from the 30-second firing, the design

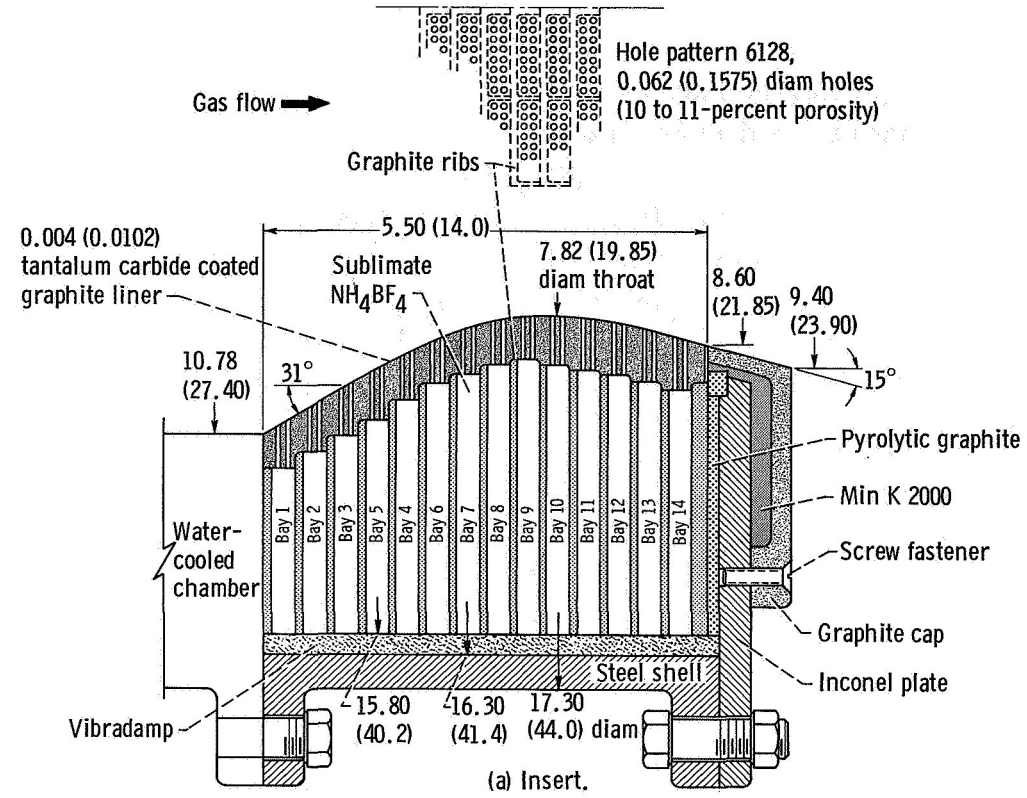

(a) Insert.

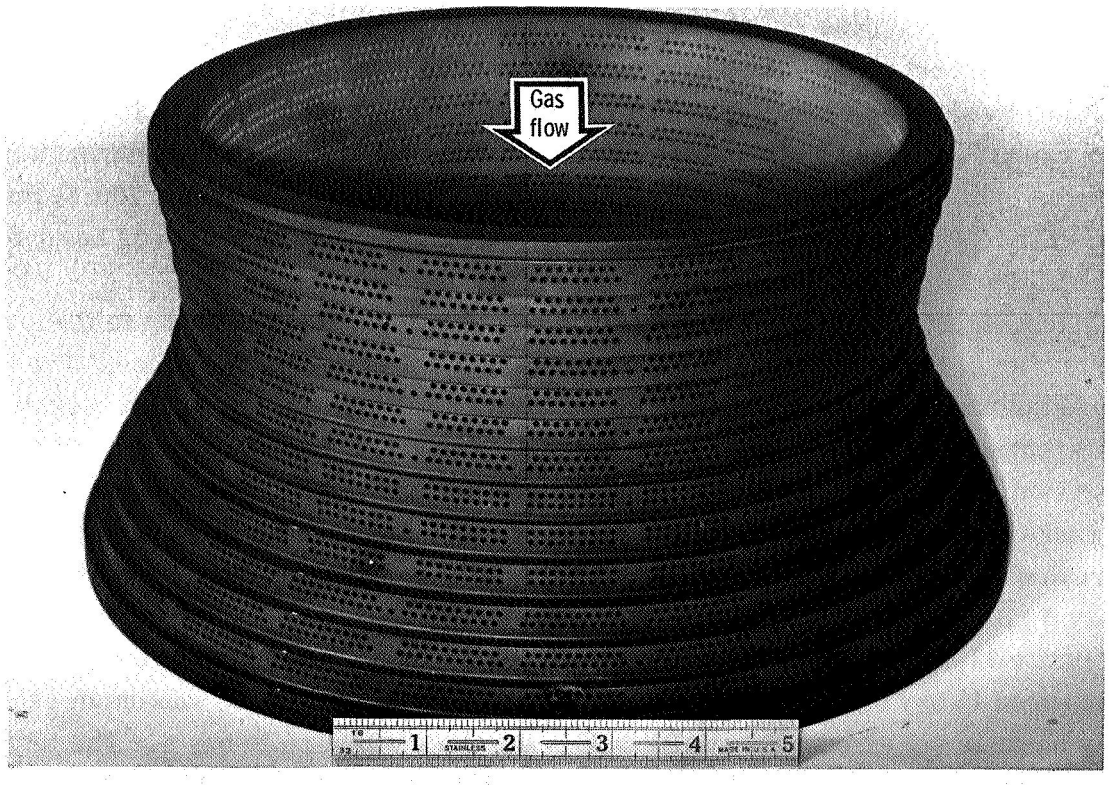

(b) Liner before assembly.

Figure 11. - Nozzle 4A; tantalum carbide coated graphite liner.

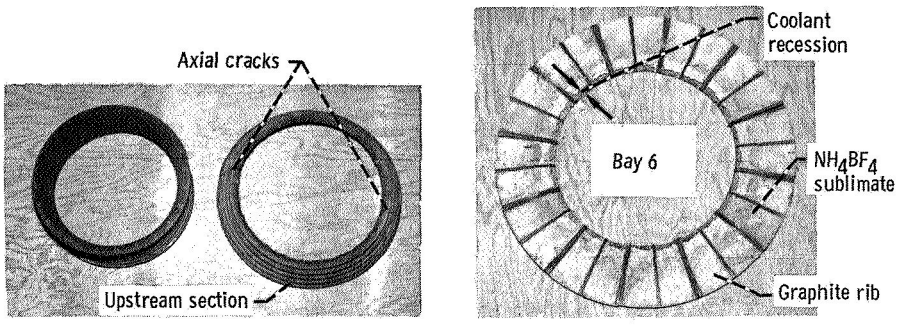

(c) Post-test photographs.

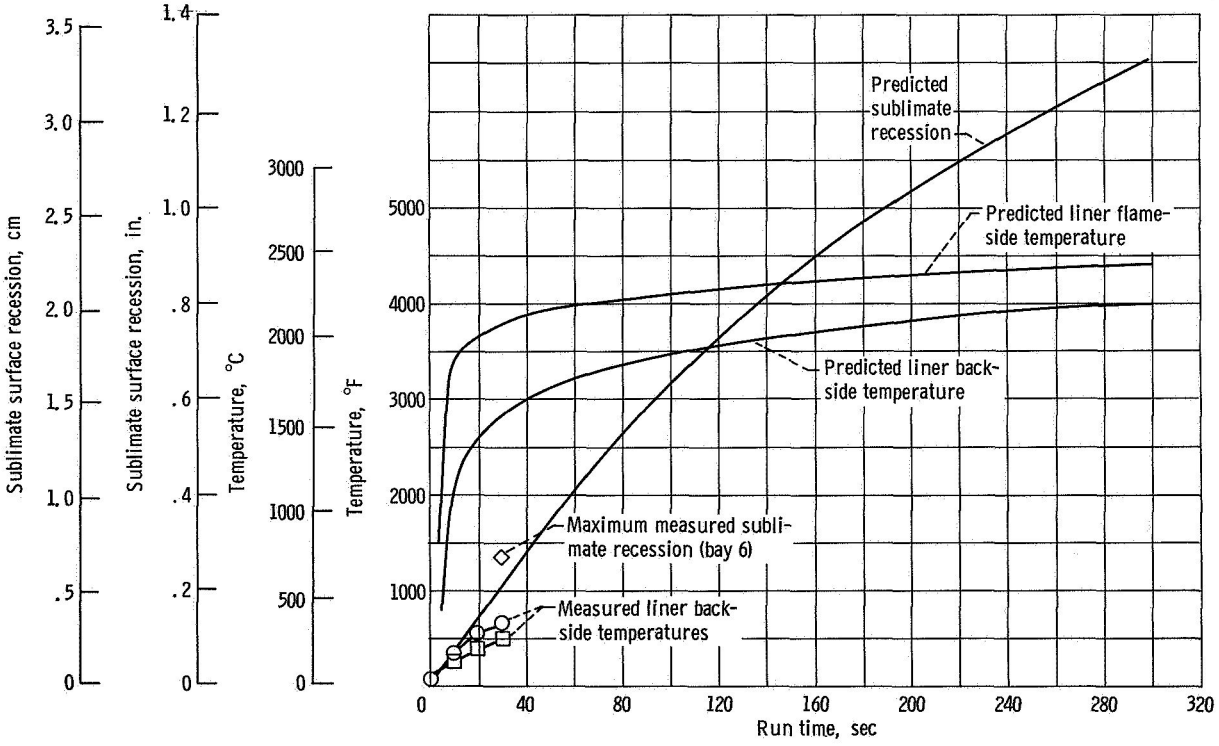

(d) Predicted and measured thermal performance and sublimate recession.

Figure 11. - Concluded.

appeared thermally conservative.

Some erosion of the tantalum carbide coating was evident around the cooling holes, especially upstream of the throat plane. The coating was intact on the rest of the surface, however.

The liner thermal stress failure may have been caused by any of the following: stress concentrations (sharp corners) on the outside of the liner, stress concentrations not accounted for in the small cooling holes, or end restraint applied by lack of clearance between the liner and fixed end plates.

The graphite cap on the Inconel end plate (fig. 11(a)) was missing following the test firing. This failure was probably caused by a combination of thermal stress and lack of support because the screw fasteners were located too far away from the point of load application.

Tantalum Carbide Coated Perforated Graphite Liner; Nozzle 4B

Using information generated during testing of nozzle 4A, nozzle 4B was designed and fabricated using as much hardware from nozzle 4A as possible. Figure 12(a) shows the new design, nozzle 4B. A new liner was required but, because the thermal performance seemed satisfactory, the hole pattern and porosity (10 to 11 percent) was the same as in nozzle 4A. The outside of the liner was machined smooth to remove stress concentrations of the original design. The liner wall thickness was decreased from 0.65 inch (1.65 cm) (nozzle 4A) to 0.38 inch (0.965 cm) (nozzle 4B) to reduce thermal stress. A tantalum carbide coating was again used to assist in oxidation protection. New graphite end plates were designed to prevent cracking. New insulation materials were used at both ends of the nozzle and around the outside of the ribs. Figure 12(a) shows the details. The end restraint on the liner was reduced by leaving an 0.010-inch (0.025-cm) gap at the upstream end and by using a soft partially cured plastic material at the downstream end. A new supply of coolant replaced that used during the initial test. The same graphite ribs were used wherever possible. In addition, coolant material was placed in the cooling holes and a layer of partially cured coolant, 0.010 inch (0.025 cm) thick, was applied to the inside surface of the liner. The additional material was intended to lessen the initial thermal shock applied to the liner. The steel shell and Inconel end plate for nozzle 4A were again used for nozzle 4B.

The test firing of nozzle 4B was programmed for 300 seconds to test the steady-state cooling capacity of the nozzle protection system. The firing was stopped manually when a sudden increase in the throat erosion rate was observed after approximately 90 seconds firing time. Figure 12(b) gives results from aerodynamic flow calculations, although post-test inspection of the nozzle revealed that the liner was completely missing and that

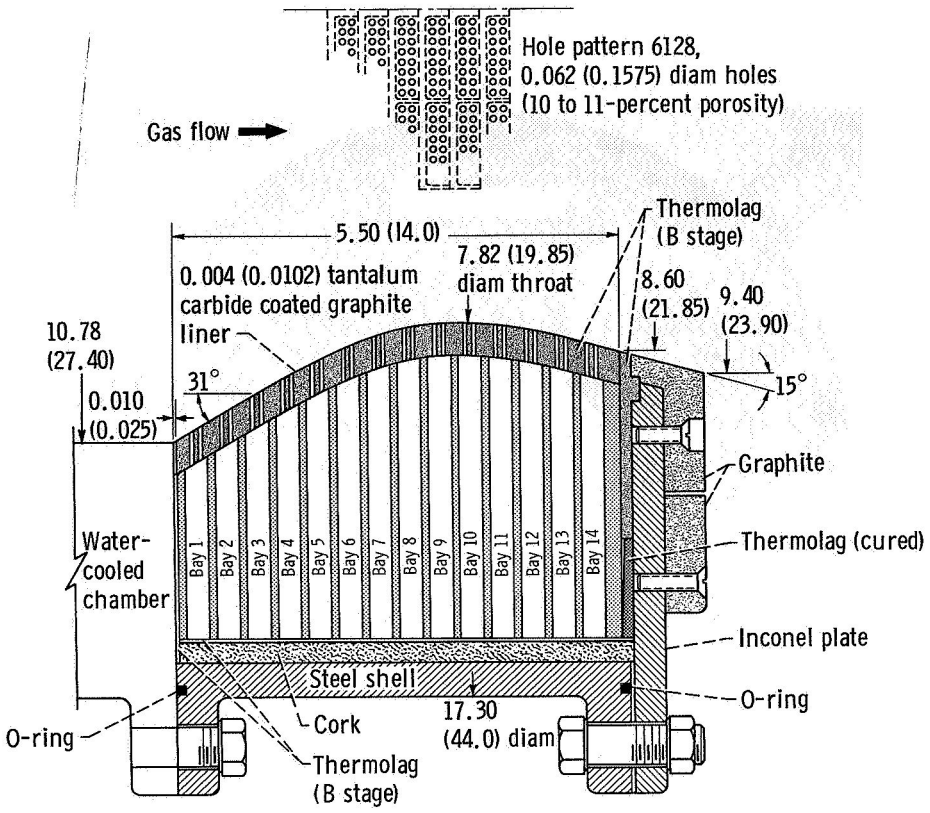

(a) Insert

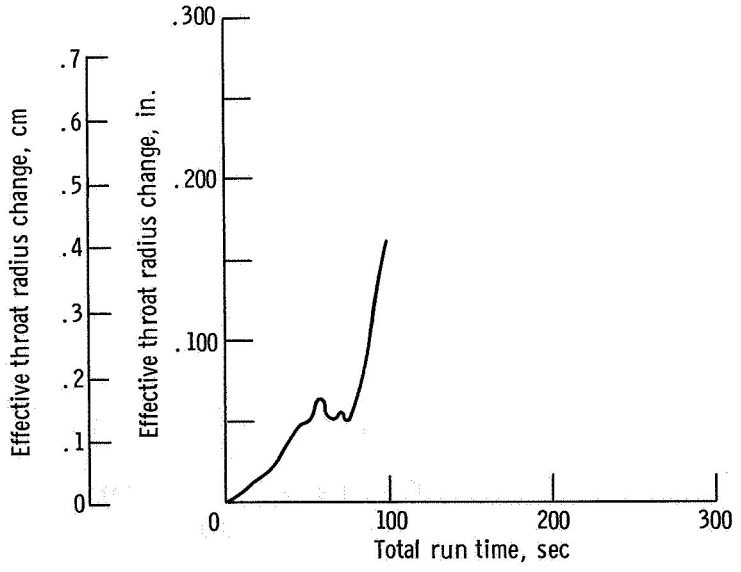

(b) Throat erosion of cooling concept.

Figure 12. - Nozzle 4B; tantalum carbide coated graphite liner with NH_4BF_4 coolant.

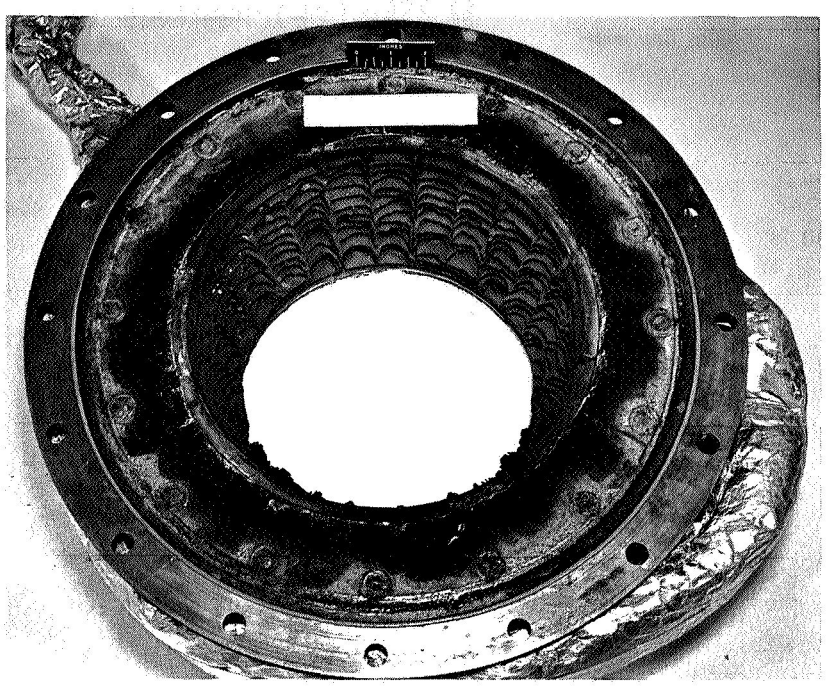

(c) Post-test photograph.

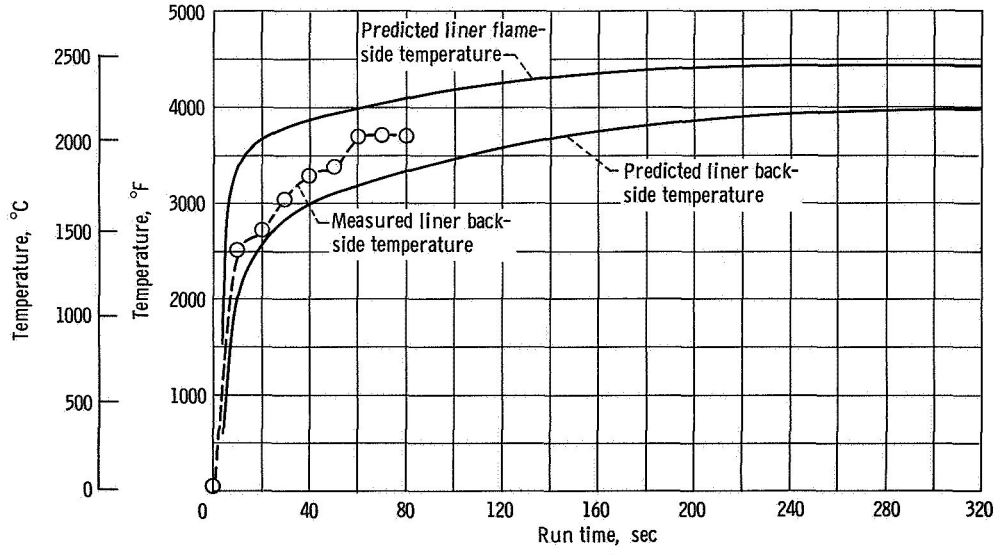

(d) Predicted and measured thermal performance.

Figure 12. - Concluded.

the ends of the ribs containing the coolant were exposed. The extent of the damage is illustrated in figure 12(c). Motion pictures of the nozzle during firing showed that erosion began around the holes in the liner. The upstream rows were affected first. The unaffected areas of the liner between the holes failed structurally as erosion progressed. The combination of oxidation and structural failure proceeded from upstream to the throat plane. The rapid increase in erosion rate after 75 seconds occurred as the liner was eroding at the throat plane. The basic failure was preferential oxidation around the cooling holes due either to their orientation and associated turbulence or possible chemical reactions with the coolant.

The measured and manufacturer's predicted liner backside temperatures are shown in figure 12(d) for the throat plane over bay 10. The measured temperatures were higher than for nozzle 4A. This could have been due to the decreased liner mass or, more likely, better contact between the thermocouples and the liner. The measured temperatures higher than predicted indicate the flame side liner wall temperature could also have been 300° F (165° C) higher than predicted. The high wall temperature, together with the erosion of the liner, shows that the coolant did not adequately cool the liner. The modifications to the graphite end cap design for nozzle 4B prevented structural failure in this area so that no change was required for these parts.

80-Percent Tungsten - 20-Percent Silver Perforated Washer Liner; Nozzle 4C

Based on the results of the first two tests, it was concluded that a significant redesign of the nozzle was required to evaluate the usefulness of the concept for long-duration engine firings.

The design of nozzle 4C is shown in figure 13(a). The hole pattern was revised to provide more even coolant-gas distribution. The liner porosity was reduced to 3 to 4 percent to increase coolant-gas pressure and to provide a higher coolant-injection velocity. Copper foam was added to the coolant material to increase heat transfer to the coolant and, therefore, increase coolant gas flow rate. The liner design was changed to a stacked washer configuration to reduce axial thermal stress. The silver infiltrated tungsten liner material was chosen because previous work (ref. 7) indicated that erosion was a time-temperature dependent oxidation problem. It was hoped the transpiring coolant would hold the temperature level of the liner below the oxidation threshold temperature of tungsten - silver (W - Ag) for a 300-second firing.

The test firing of nozzle 4C was programmed for 300 seconds. The firing was ended manually after 166 seconds when high-frequency combustion instability was detected in the chamber. Post-test inspection revealed that the liner washers were not cracked but

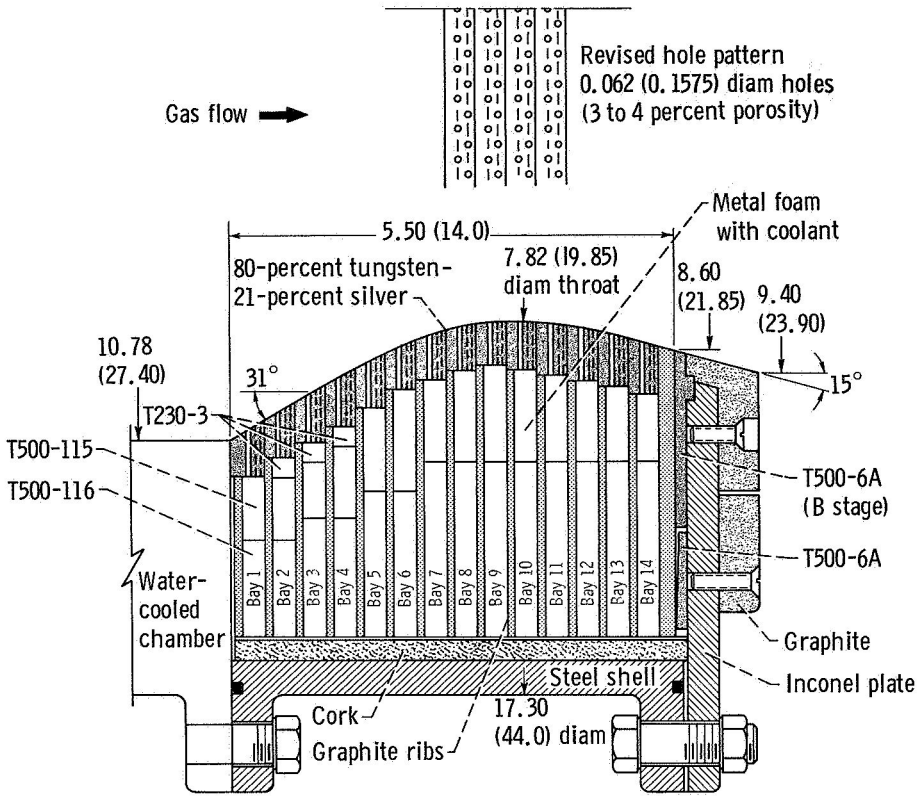

(a) Insert.

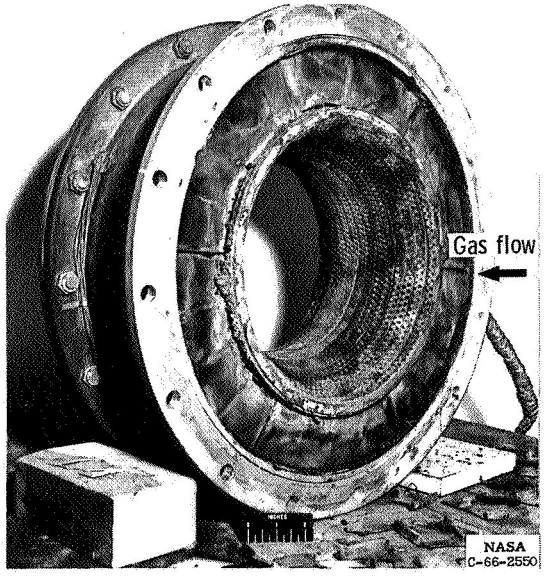

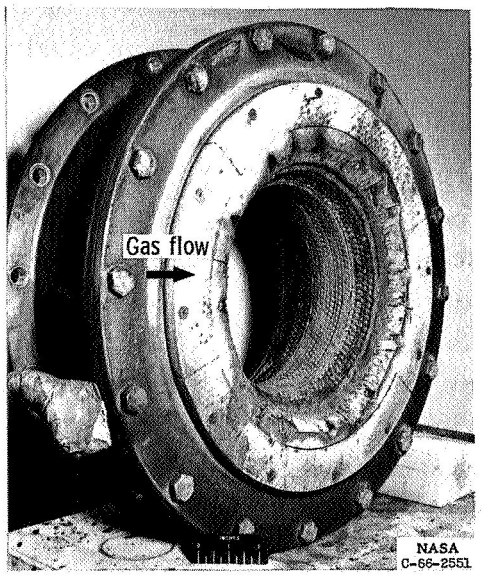

(b) Post-test photographs.

Figure 13. - Nozzle 4C; 80-percent tungsten - 20-percent silver perforated washer liner: cooling concept.

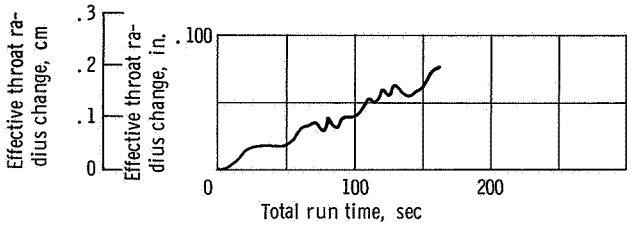

(c) Throat erosion.

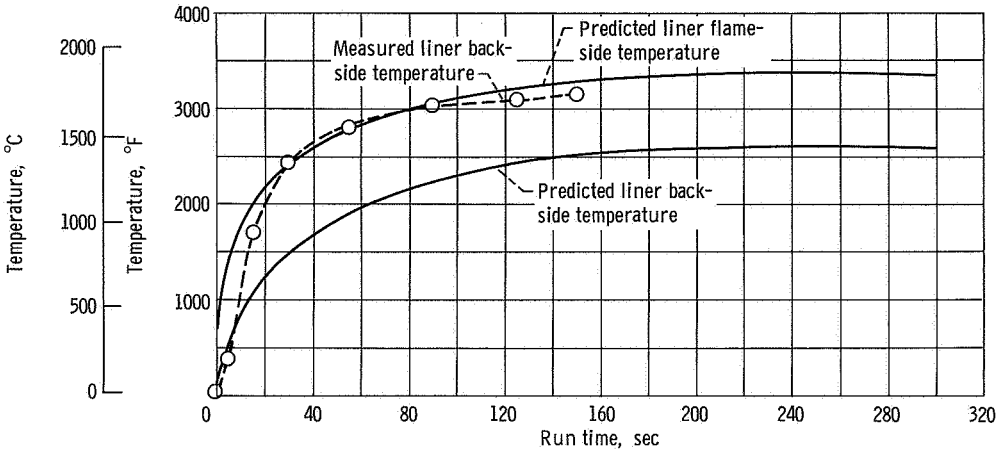

(d) Predicted and measured thermal performance.

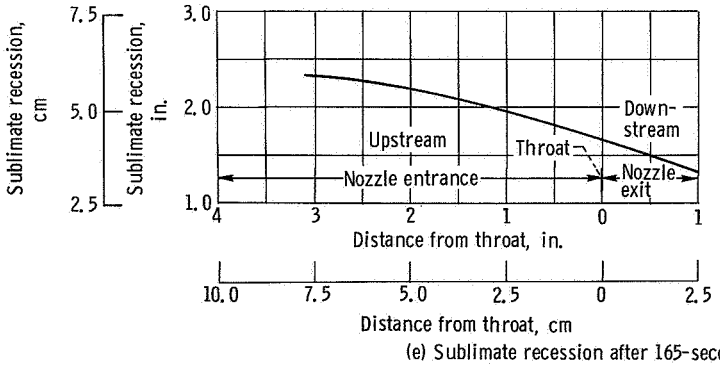

(e) Sublimate recession after 165-second firing.

Figure 13. - Concluded.

that erosion was appreciable, especially around the coolant holes. Post-test photographs of the liner are given in figure 13(b). The throat erosion is plotted on figure 13(c) along with similar data for the previous design. The overall erosion rate is of the same magnitude as erosion of uncooled tungsten silver (ref. 7). The erosion upstream of the throat and around the cooling holes was more severe than at the throat. The predicted liner temperatures are compared with measured liner backside temperatures on figure 13(d). The actual temperature is seen to be about 600° F (330° C) higher than predicted at the end of the test firing. All these facts indicate that the coolant did not protect the liner as intended. The amount of coolant loss is plotted in figure 13(e). A significant amount of coolant was used during the limited test. Almost 2.5 inches (6.35 cm), or more than 50 percent, of the available coolant was depleted in the upstream section of the nozzle. Where the coolant was gone, the copper foam was also gone. It was probable that some of the coolant gases were released because of heat soak after engine shutdown.

The coolant material used in the three designs tested was apparently not sufficient to prevent oxidation of the liners in the test environment for the design duration. Structural and heat-transfer problems with a perforated liner are complex; however, cracking of the liner, which was a problem with the first nozzle design, was not encountered with the material and washer construction of nozzle 4C. Lack of adequate cooling from the coolant reservoir could be due to any of the following: (1) heat conduction into the coolant reservoir was not sufficient to generate gas pressure required to force adequate coolant gases into the combustion stream, (2) coolant gases that were generated could have reacted chemically with the liner material and contributed to the problem rather than solving it, (3) coolant gases generated could have found low-pressure leakage paths behind the liner, rather than being forced into the gas stream or were released only after engine shutdown.

Possible improvements in the design would include design of continuous heat paths finely distributed into the coolant material to assure proper vaporization. Pyrolytic graphite would also provide better heat conduction once a continuous path was established. Use of copper foam was an attempt to maintain intimate contact between the coolant material and the heat source to provide better vaporization. Other material combinations and heat-transfer mechanisms could be investigated. A design where coolant gases could only move in the proper path would help assure full coolant utilization. Turbulence and increased heat transfer in the coolant hole area could possibly be controlled by orienting the holes differently, changing their geometry, or using a porous liner rather than discrete holes.

SUMMARY OF RESULTS

Three throat inserts and an active cooling concept were evaluated in a 7.82-inch (19.8-cm) throat-diameter rocket engine using nitrogen tetroxide and a blend of 50-percent hydrazine with 50-percent unsymmetrical dimethyl hydrazine earth storable propellants. Eliminating throat erosion while maintaining structural integrity for an extended duty cycle was more difficult in this scale than in smaller size inserts.

Structural failure led to throat erosion after about 60 seconds firing time for throat inserts of magnesium oxide reinforced with steel or Inconel honeycomb. The same type of cracking had been experienced with small-scale inserts (ref. 6).

JT0992, a hafnium carbide, silicon carbide, graphite composite, provided erosion protection as a throat insert for 140 seconds. Subsequent erosion due to oxidation was caused by loss of the protective oxide formed during firing. For small-scale inserts, the oxide remained in place and erosion was minimized without cracking. Cracking occurred in the large-scale with significantly higher erosion rates. After firing, the insert was not suitable for refire because of the high erosion and severe cracking. Smaller size inserts of the same material did not fail structurally. The difference could have been due to higher thermal stresses and/or weaker material in the large size insert. A means for assuring the retention of a protective oxide on this type of material composite is required to prevent erosion.

Relative to the active cooling concept, a tantalum carbide coated perforated graphite throat liner, with a coolant reservoir, cracked axially and circumferentially during a 30-second test firing. A second nozzle modified in an attempt to eliminate structural failure, but with a liner similar to that of the first nozzle, eroded because of oxidation and failed catastrophically after approximately 80 seconds of firing. A third nozzle with a perforated tungsten-silver throat liner was tested for 166 seconds with nominal throat erosion. Erosion rate, due to oxidation, was generally similar to uncooled tungsten-silver nozzles tested previously. The coolant material (ammonium fluoroborate) from the reservoir apparently failed to provide adequate cooling in any of the designs tested. A possible cause could have been that coolant gases were not generated in sufficient quantity or at a high enough pressure to be forced into the combustion stream. Coolant gases could also have found low-pressure leakage paths behind the liner or escaped only after engine shutdown at reduced pressures.

Lewis Research Center,
National Aeronautics and Space Administration,
Cleveland, Ohio, July 11, 1968,
128-31-03-02-22.

APPENDIX - SYMBOLS

A_e	rocket nozzle exit area, in.^{2}; cm^2
A_t	throat area, in.^{2}; cm^2
C_d	nozzle discharge coefficient 0.994
C^*	characteristic exhaust velocity
C^*_{theo}	theoretical characteristic exhaust velocity (shifting equilibrium)
D_e	rocket nozzle exit diameter, in.; cm
F	thrust, lb force; N
F_{vac}	vacuum thrust, $F + P_o D_e^2 \pi/4$, lb force; N
g	gravitational constant, ft/sec^2; m/sec^2
I_{vac}	vacuum impulse, F_{vac}/W_p, sec
L^*	characteristic chamber length (V_c/A_t), in.; cm
O/F	oxidant-fuel ratio, W_{ox}/W_f
P_c	chamber pressure measured at injector, psia; kN/m^2
$P_{c,corr}$	corrected chamber pressure (total pressure at rocket throat) φP_c, psia; kN/m^2
P_o	altitude pressure surrounding engine, psia; kN/m^2
ΔR_{eff}	effective throat radius change, $R_t - R_i$, in.; cm
R_i	initial throat radius, in.; cm
R_t	throat radius, $\sqrt{\frac{\eta C^* C^*_{theo} W_p}{\pi g P_{c,corr} C_d}}$, in.; cm
V_c	rocket chamber volume to throat plane, in.^{3}; cm^3
W_f	fuel weight flow, average $(W_{f,1} + W_{f,2})/2$, lb/sec; kg/sec
W_{ox}	oxidant weight flow, average $(W_{ox,1} + W_{ox,2})/2$, lb/sec; kg/sec
W_p	total propellant flow, $W_{ox} + W_f$, lb/sec; kg/sec
ϵ	nozzle expansion area ratio (A_e/A_t)
ηC^*	characteristic velocity efficiency, $I_{vac}/C_{F_{vac}}$
$\eta C_{F,vac}$	vacuum thrust coefficient efficiency (0.983)
ηI_{vac}	vacuum impulse efficiency, $I_{vac}/I_{vac,theo}$ equilibrium
φ	correction factor for measured chamber pressure at injector to chamber total pressure at the throat (0.946)

REFERENCES

1. Mitchel, Barry J.: Ablative Plastics Characterization. Rep. AUSSD-0204-67-RR, Avco Corp. (AFML-TR-67-176, DDC No. AD-821572L), Sept. 1967.

2. Lubowitz, H. R.; Burns, E. A.; and Dubrow, B.: Investigation of Resin for Improved Ablative Materials. Rep. 4176-6014-50-000, TRW Systems (NASA CR-54471), Apr. 1, 1966.

3. Butler, J. M., et al: Research on Ablative Compositions. Second Semi-annual Summ. Rep., Monsanto Research Corp., 1965. (Contract DA-31-124-ARO (D) - 279, ARPA Order No. 533.)

4. Peterson, Donald A.: Experimental Evaluation of High-Purity-Silica Reinforced Ablative Composites as Nozzle Sections of 7.8-inch (19.8-cm) Diameter Throat Storable-Propellant Rocket Engine. NASA TM X-1391, 1967.

5. Winter, Jerry M.; Plews, Larry D.; and Johnston, James R.: Experimental Evaluation of Throat Inserts in a Storable-Propellant Rocket Engine. NASA TM X-1266, 1966.

6. Winter, Jerry M.; and Peterson, Donald A.: Development of Improved Throat Inserts for Ablative Rocket Engines. NASA TN D-4964, 1968.

7. Winter, Jerry M.; and Peterson, Donald A.: Experimental Evaluation of 7.82-Inch (19.8-cm) Diameter Throat Inserts in a Storable-Propellant Rocket Engine. NASA TM X-1463, 1968.

NASA-Langley, 1969 —— 28 E-4550

"The aeronautical and space activities of the United States shall be conducted so as to contribute . . . to the expansion of human knowledge of phenomena in the atmosphere and space. The Administration shall provide for the widest practicable and appropriate dissemination of information concerning its activities and the results thereof."

—NATIONAL AERONAUTICS AND SPACE ACT OF 1958

NASA SCIENTIFIC AND TECHNICAL PUBLICATIONS

TECHNICAL REPORTS: Scientific and technical information considered important, complete, and a lasting contribution to existing knowledge.

TECHNICAL NOTES: Information less broad in scope but nevertheless of importance as a contribution to existing knowledge.

TECHNICAL MEMORANDUMS: Information receiving limited distribution because of preliminary data, security classification, or other reasons.

CONTRACTOR REPORTS: Scientific and technical information generated under a NASA contract or grant and considered an important contribution to existing knowledge.

TECHNICAL TRANSLATIONS: Information published in a foreign language considered to merit NASA distribution in English.

SPECIAL PUBLICATIONS: Information derived from or of value to NASA activities. Publications include conference proceedings, monographs, data compilations, handbooks, sourcebooks, and special bibliographies.

TECHNOLOGY UTILIZATION PUBLICATIONS: Information on technology used by NASA that may be of particular interest in commercial and other non-aerospace applications. Publications include Tech Briefs, Technology Utilization Reports and Notes, and Technology Surveys.

Details on the availability of these publications may be obtained from:

SCIENTIFIC AND TECHNICAL INFORMATION DIVISION
NATIONAL AERONAUTICS AND SPACE ADMINISTRATION
Washington, D.C. 20546